



HAL
open science

The *C. elegans* HP1 homologue HPL-2 and the LIN-13 zinc finger protein form a complex implicated in vulval development

Vincent Coustham, Cécile Bedet, Monier Karine, Sonia Schott, Karali Marianthi, Francesca Palladino

► To cite this version:

Vincent Coustham, Cécile Bedet, Monier Karine, Sonia Schott, Karali Marianthi, et al.. The *C. elegans* HP1 homologue HPL-2 and the LIN-13 zinc finger protein form a complex implicated in vulval development. *Developmental Biology*, 2006, 297, pp.308-322. ensl-00182491

HAL Id: ensl-00182491

<https://ens-lyon.hal.science/ensl-00182491>

Submitted on 26 Oct 2007

HAL is a multi-disciplinary open access archive for the deposit and dissemination of scientific research documents, whether they are published or not. The documents may come from teaching and research institutions in France or abroad, or from public or private research centers.

L'archive ouverte pluridisciplinaire **HAL**, est destinée au dépôt et à la diffusion de documents scientifiques de niveau recherche, publiés ou non, émanant des établissements d'enseignement et de recherche français ou étrangers, des laboratoires publics ou privés.

The *C. elegans* HP1 homologue HPL-2 and the LIN-13 zinc finger protein form a complex implicated in vulval development

Vincent Coustham, Cécile Bedet, Karine Monier, Sonia Schott,
Marianthi Karali, Francesca Palladino *

Laboratoire de Biologie Moléculaire de la Cellule, Ecole Normale Supérieure de Lyon, 46 allée d'Italie, 69007 Lyon, France

Received for publication 21 December 2005; revised 10 April 2006; accepted 11 April 2006

Available online 23 May 2006

Abstract

HP1 proteins are essential components of heterochromatin and contribute to the transcriptional repression of euchromatic genes via the recruitment to specific promoters by corepressor proteins including TIF1 and Rb. The *Caenorhabditis elegans* HP1 homologue HPL-2 acts in the “synMuv” (synthetic multivulval) pathway, which defines redundant negative regulators of a Ras signaling cascade required for vulval induction. Several synMuv genes encode for chromatin-associated proteins involved in transcriptional regulation, including Rb and components of the Mi-2/NuRD and TIP60/NuA4 chromatin remodeling complexes. Here, we show that HPL-2 physically interacts *in vitro* and *in vivo* with the multiple zinc finger protein LIN-13, another member of the synMuv pathway. A variant of the conserved PXVXL motif found in many HP1-interacting proteins mediates LIN-13 binding to the CSD of HPL-2. We further show by *in vivo* localization studies that LIN-13 is required for HPL-2 recruitment in nuclear foci. Our data suggest that the LIN-13/HPL-2 complex may physically link a subset of the Rb related synMuv proteins to chromatin.

© 2006 Elsevier Inc. All rights reserved.

Keywords: *C. elegans*; HP1; Chromatin; LIN-13; Vulva

Introduction

HP1 proteins are a highly conserved family of proteins which directly contribute to the higher order packaging of chromatin by binding to modified histones (Li et al., 2002). All HP1 proteins are structurally related and characterized by the presence of two conserved domains, an N-terminal chromo domain (CD) separated by a variable hinge region from a C-terminal-related domain termed the chromo shadow domain (CSD). The CD is responsible for binding to methylated histone H3-K9, while the CSD is required for dimerization and most protein–protein interactions within the nucleus (Eissenberg, 2001). Many of these interactions play an important role in directing heterochromatin formation and/or gene silencing. A large number of the CSD interaction partners contain a PXVXL pentapeptide motif, including the

transcription intermediary factor TIF1, the TBP-associated factor TAFII130, and the large subunit of chromatin assembly factor 1 (CAF-1) (Le Douarin et al., 1996; Murzina et al., 1999; Vassallo and Tanese, 2002). These results suggest that HP1 proteins function as adapters, bringing together different proteins in multiprotein complexes via protein–protein interactions with the CD and CSD. The multiple interactions of the CSD underscore the complexity of HP1 dynamics. However, it remains to be established how many partners HP1 has under a given set of conditions and how important these interactions are in different cellular contexts. The *Caenorhabditis elegans* vulva is a simple, well-described system particularly suited to study how chromatin regulation can function in a specific developmental pathway. Previously, we showed by RNAi that the *C. elegans* HP1-like protein HPL-2 contributes to vulval development by acting in the Rb related synMuvB pathway antagonistic to the Ras-mediated signal transduction pathway responsible for vulval cell fate determination (Couteau et al., 2002). In addition to LIN-35Rb, synMuvB genes encode homologues of the class I

* Corresponding author. Fax: +33 4 72728080.

E-mail address: francesca.palladino@ens-lyon.fr (F. Palladino).

histone deacetylase HDA-1, EFL-1/E2F, DPL-1/DP (Ceol and Horvitz, 2001; Lu and Horvitz, 1998) and counterparts of the NuRD nucleosome remodeling and histone deacetylase complex (Solari and Ahringer, 2000; von Zelewsky et al., 2000). Based on the identity of the cloned class B synMuv genes, it has been proposed that they remodel chromatin and repress transcription of genes important for vulval cell fate specification. More recently, a TIP60/NuA4-like complex was also implicated in the negative regulation of Ras signaling during vulval cell fate specification (Ceol and Horvitz, 2004). These results strongly suggest that different chromatin remodeling and modification complexes may cooperate in the same developmental pathway. To gain insight into the specific role played by HPL-2 in vulval cell fate determination, we carried out a two-hybrid screen to identify potential partners. One of the proteins identified is the LIN-13 zinc finger protein, another member of the synMuvB pathway (Melendez and Greenwald, 2000; Ferguson and Horvitz, 1989; Thomas et al., 2003). The interaction between the two proteins was confirmed in vivo and depends on the CSD of HPL-2 and a conserved HP1 binding motif in the N-terminus of LIN-13. Finally, we show that the localization of HPL-2 in nuclear foci is completely dependent on *lin-13* but not other synMuvB genes such as *lin-35* and *lin-9*. Altogether, these results suggest the existence of a hierarchy in the recruitment of the Rb-related synMuvB complex to chromatin.

Materials and methods

Yeast strains and media

Strains used are the following: CG1945 (*MATa gal4-542 gal80-538 ade2-101 his3-200 leu2-3,112 trp1-901 ura3-52 lys2-801 [URA3::GAL4 17mers (X3)-CyC1TATA-lacZ] LYS2::GAL1UAS-GAL1TATA-HIS3 CYH^{RS}*) (gift from L. Segalat); Y187 (*MATα gal4Δ gal480Δ ade2-101 his3 leu2-3,112 trp1-901 ura3-52 URA3::UASGAL1-lacZ met⁻*); and PJ69-4a/α (*MATA/α trp-1-901 leu2-3,112 ura3-52 his3-200 gal4Δ gal480Δ LYS2::GAL1-HIS3 GAL2-ADE2 met2::GAL7-lacZ*). Basic methodology for yeast was as described by Fink (1991).

C. elegans strains and genetics

Strains were maintained according to the standard protocol (Brenner, 1974). The following mutant alleles were used: LGI *lin-35(n745)*; LGIII *hpl-2(ok916)*, *hpl-2(ok917)*, *hpl-2(tm1489)*, *lin-13(n388)*, *unc-32(e189)*, *unc-49(e407)*, *dpy-17(e164)*; X *lin-15(n767)*. *ok916*, *ok917* and *tm1489* alleles were backcrossed four times prior to analysis and the presence of the deletion allele confirmed by PCR analysis. The *hpl-2* wild-type sequence fully rescued synMuv and synthetic lethal phenotypes and partially rescued the sterility of all three alleles. For expression studies *lin-39::GFP* (gift from A. Hajnal) and *qls56[lag-2::GFP]* were used. To construct the *lin-13(n388)dpy-17(e164)hpl-2(tm1489)unc-49(e407)* strain, *lin-13(n388)unc-32(e189)* worms were crossed with *dpy-17(e164);lin15(n767)* males. Recombinant *lin-13(n388)dpy-17(e164);lin15(n767)* were selected based on the Muv phenotype in their progeny at 20°C and then crossed with *unc-49(e407)hpl-2(tm1489)* males. *lin-13(n388)dpy-17(e164)hpl-2(tm1489)unc-49(e407)+* recombinants were selected as Dpy Unc animals segregating in their progeny at 20°C. Loss of the *lin15(n767)* allele was confirmed by duplex PCR (M. Koelle laboratory protocol) using the following primers: for 5'-GGGAAGGTTACGTCGAACAC-3'; rev1 5'-GATTCGTCGATGGAGG-CACC-3'; rev2 5'-GCCTCGTCGGCAATTGAATG-3'. The presence of the *tm1489* deletion in *lin-13 hpl-2* mutants was confirmed by duplex PCR using the

following primers: for1 (outside deletion) 5'-TACATGCAACAAACCGCGCT-3'; for2 (inside deletion) 5'-GACAGTATAAGTTCCCGAC-3'; rev 5'-GTTTACCAGCTTTTCCGTGTG-3', followed by sequencing using both outside primers described below. The presence of the *lin-13(n388)* C to T substitution was confirmed by sequencing.

Two-hybrid screen

The full-length *hpl-2a* cDNA was subcloned into plasmid pAS2.1 (Clontech) to create pCV1. The two-hybrid screen was performed by mating, as described (Fromont-Racine et al., 1997) using yeast strains CG1945 and Y187 and the *C. elegans* cDNA library λACT-RB2 (Durfee et al., 1993; Elledge et al., 1991). Positive interactions were selected using the *lacZ* and *HIS3* reporter genes on HIS selection plates supplemented with 10 mM 3-AT. Interacting partners were confirmed by re-transformation in PJ69-4a, mating with a PJ69-4a carrying either pAS2.1 or pCV1 vectors, and selection for expression of *ADE2* and *HIS3* reporters. For directed two-hybrid assays, baits were transformed in PJ69-4a strain and mated with strain PJ69-4a carrying preys cloned in the pGADT7 vector (Clontech).

PCR of *hpl-2* fragments

For domain mapping experiments, specific fragments of *hpl-2a* cDNA sequence were amplified by PCR with oligonucleotides designed at following positions: CD, for 5'-ATGTCGAGCAAATCAACAAA-3', rev 5'-CTCAAACCTCGTCCAACATCTC-3'; CSD, for 5'-GAAACGAATCAAATGACAAATTC-3', rev 5'-TTAAAGCTCGTCGGCTTTTGG-3'; Hinge, for 5'-AGGGAATTTTCAAAGAGAGAG-3', rev 5'-CTCTTTTCAICTT-TATCCTCTTC-3'; Hinge+CSD, for 5'-AGGGAATTTTCAAAGAGAGAG-3', rev 5'-TTAAAGCTCGTCGGCTTTTGG-3'. For HPL-2Δ, primers used were for 5'-ATGTCGAGCAAATCAACAAA-3', rev 5'-ACTGTTTACCTCTTCGTCGG-3'. For this last construct, a stop codon was added at nucleotide position 453, corresponding to the 5' breakpoint of *ok916* and *ok917* deletion alleles. For LIN-13, point mutations were introduced resulting in a change at position 442 (V to D) and position 444 (V to E) using the Quickchange Site-directed Mutagenesis kit (Stratagene) on the cDNA isolated from two-hybrid experiment. Primers used were 5'-GAACCATCTTGTC AACCGTTGGATCCG-GAGGTTGCTTACTTCCCAAACCG-3' and 5'-CGGTTTTGGGAAGTAAG-CAACCTCCGGATCCAACGGTTGACAAGAATGGTTC-3'. The presence of the point mutations was confirmed by sequencing.

Deletion mapping

Total genomic DNA was extracted from mixed-stage populations of *ok916* and *ok917* mutant worms. Oligonucleotides were designed as described by the *C. elegans* Knockout Consortium. Nested PCR was performed using BIO-X-ACT polymerase (Bioline). The *tm1489* deletion predicted by the National BioResource Project was confirmed by sequencing using primers described below.

Reverse transcriptase - polymerase chain reaction (RT-PCR) and sequencing

Total RNA was isolated from mixed-stage populations of homozygous *ok916*, *ok917* and N2 worms using Trizol reagent (Sigma). First-strand synthesis and RT-PCR were performed in a single reaction using the Access RT-PCR Kit (Promega). Oligonucleotides were designed at the following positions: 4799–4819 (for exon 2, 5'-AGGACAACGTGTTTCATGGTGG-3'); 7011–7030 (rev exon 5-2B, 5'-CTTCAGTCATCTCAACGTCC-3'); 7617–7638 (rev exon 6-2B, 5'-ATCATCGTCTGGTACAGTGTGCG-3').

RNAi

RNAi injection and feeding experiments were carried out as described (Fire et al., 1998; Kamath and Ahringer, 2003). When necessary, to produce a weaker RNAi effect, the concentration of IPTG in feeding plates was reduced to 0.1 mM IPTG. Induction was 12 h at room temperature. Most RNAi feeding clones were obtained from Geneservice. For the *lin-13*

feeding clone, the cDNA sequence of *lin-13* obtained in the two-hybrid screen was subcloned into the L4440 feeding vector and transformed into HT115. RNAi of *lin-13* by feeding resulted in the same range of highly penetrant temperature-sensitive phenotypes previously reported by injection (Melendez and Greenwald (2000), including sterility, evl (everted vulva), and Muv in combination with class A synMuv mutations at 15–20°C, and larval arrest at 25°C (data not shown). *lin-15A*-specific RNA for injection was prepared as previously described (von Zelewsky et al., 2000). For *hpl-2::GFP* localization studies, embryos were dissected from gravid mothers derived either from L1 larvae grown on RNAi feeding plates, or from injected L4 larvae. For *lin-9* and *lin-35* feeding, the efficacy of RNAi was measured by placing *lin-15A* mutant animals on these plates and looking for 100% Muv animals. For *lin-13*, *mys-1*, *trr-1*, *hda-1* and *let-418*, RNAi feeding yielded the phenotypes previously described (Kamath and Ahringer, 2003).

GST pull-down assay

GST-HPL-2 fusion protein expressed in *E. coli* using the full-length *hpl-2a* cDNA cloned in pGEX-KG (Pharmacia) was immobilized on glutathione-agarose beads (Sigma). Proteins subcloned in pGADT7 vector were produced and labeled with [³⁵S]methionine using the TNT T7-coupled reticulocyte lysate system (Promega). Beads were incubated with in vitro produced proteins 2 h at 4°C in PBS with 0.05–0.2% Triton, washed and analyzed on SDS-PAGE.

Preparation of embryo extracts

Hermaphrodites carrying a rescuing LIN-13::GFP transgene were grown in liquid as described (Mains and McGhee, 1999). Embryos recovered following alkaline hypochlorite treatment of gravid adults were recovered by centrifugation, resuspended in 5 volumes of cold TNT buffer (Tris–HCl 50 mM pH = 8; NaCl 150 mM; Triton X-100 1% + protease inhibitor cocktail (Complete EDTA, Roche Applied Science, plus 1 mM PMSF) and sonicated on ice. Lysates were spun at high speed for 10 min at 4°C, and supernatants were collected and assayed for protein concentration using Bradford reagent (Bio-Rad Laboratories). Protein concentration of the LIN-13::GFP embryonic lysate was ≈5 mg/ml.

Immunoprecipitation and Western blot

3 μl of rabbit polyclonal affinity purified anti-HPL-2 antibody or preimmune serum, or 4 μg of anti-GFP (Clones 7.1 and 13.1, Roche Applied Science) or anti-FLAG (M2 monoclonal, Sigma) antibodies were added to 250 μl of LIN-13::GFP embryonic lysate diluted twice in TNT buffer. Samples were incubated at 4°C for 1 h, 30 and 50 μl of a 1:1 slurry of protein A–sepharose (Amersham Bioscience) or protein G–sepharose (Sigma) beads were added. Samples were incubated another 2 h at 4°C. The beads were washed two times in 1 ml of buffer A (10 mM Tris–HCl pH = 8; 150 mM NaCl; 0.5% T X-100), two times in 1 ml of buffer B (10 mM Tris–HCl pH = 8; 500 mM NaCl; 0.5% T X-100), and one time in 1 ml of buffer C (10 mM Tris–HCl pH = 8). Proteins were resolved by SDS-PAGE followed by Western blot analysis. Primary antibodies were rabbit affinity purified anti-HPL-2 developed in the lab and diluted at 1:2000 or anti-GFP (Roche) diluted at 1:1000. Secondary antibodies were ImmunoPure Recomb Protein A–Peroxidase Conjugated (1:15,000, Pierce) or an anti-mouse IgG (from sheep) conjugated to peroxidase (1:10,000; Amersham Bioscience). Proteins were visualized using a chemiluminescent reagent kit (Super Signal, Pierce).

Construction of *hpl-2::RFP*

hpl-2::RFP was constructed by replacing the GFP insertion in pFG2 (Couteau et al., 2002) with a monomeric RFP fragment from pRSET B (Invitrogen). Transgenic worms were generated as described previously (Mello et al., 1991). For colocalization experiments, *hpl-2::RFP* and a rescuing *lin-13::GFP* construct (gift of I. Greenwald) were coinjected with pRF4 to generate transgenic worms.

hpl-2::GFP acquisition, restoration and analysis

Number of nuclear HPL-2-GFP foci were counted in nuclei of live embryos fed with RNAi against different synMuv genes. To compare number of foci in equivalent conditions, analyses were restricted to HPL-2::GFP embryos containing between 60 and 80 cells (due to GFP intensity variation in embryos). Parameters of image acquisition, restoration, and analysis were kept constant for embryos issued of various genetic backgrounds. Image stacks of 50 sections of whole HPL-2-GFP embryos were acquired every 0.3 μm, using the 63× objective lens (NA = 1.4) of a motorized Zeiss Axioplan2 fluorescence microscope, equipped with a Coolsnap HQ camera, driven by Metamorph (v. 6.3). The 3D point spread function of our system was measured to restore image stacks using a 3D deconvolution procedure (set up with default parameters), available as a plugin in Metamorph. Maximum intensity projections of deconvolved sections were performed and observed with the same dynamic display to count nuclear foci. Superimposed nuclei as well as nuclei which could not be clearly visualized were not included in the analysis. In practice, approximately one-third of the nuclei revealed to be suitable for counting nuclear foci in the majority of embryos. The same individual counted the number of nuclear HPL-2-GFP foci in 160 to 641 nuclei for each genetic background issued from 7 to 27 representative embryos. Two other individuals independently confirmed the results. To take into account any variability of RNAi between embryos, the average number of foci per nucleus for each embryo was determined for each RNAi experiment. One-way analysis of variance, followed by Tukey Honest Significant Differences, was performed on the average number of foci per nucleus in each embryo. This design assigns any contribution of the variable RNAi effects between embryos to the residual error and therefore is unbiased with respect to the number of nuclei observed in each embryo. Differences between mutant genotypes and wild type were considered significant when zero was excluded from their 99.9% or 99.99% confidence interval. Computation was performed using R (<http://www.r-project.org/>).

Immunofluorescence experiments

Embryos were freeze cracked and fixed with MetOH followed by 3% paraformaldehyde at RT. Incubation was with anti-GFP mouse monoclonal antibody (Roche) and anti-H3K9Me3 rabbit polyclonal antibody (Upstate), both diluted at 1/500. Images were acquired using a Zeiss LSM510 confocal microscope and LSM510 v3.2 software.

Reporter gene expression analysis

lin-39::GFP and *lag-2::GFP* strains were crossed with *unc49(e407)hpl-2* (ok917), *unc49(e407)hpl-2(tm1489)* mutants, or placed on *lin-13*(RNAi) feeding plates.

Real-time quantitative RT-PCR

Gene expression was evaluated by real-time quantitative RT-PCR (LightCycler, Roche) using the LightCycler FastStart DNA Master SYBR Green 1 RT-PCR kit (Roche) on total reverse transcribed cDNA oligo-dT primed (First strand cDNA Synthesis Kit, Fermentas) obtained from RNA extracted from mixed stage wild-type or *hpl-2(tm1489)* worm populations grown at 25°C on 14-cm plates supplemented to 2.5% agar and 1% peptone. The measures were normalized to actin (*act-4*) RNA levels. The sequence of the primers were as follows: *act-4* for 5'-AGG-TCATCACCGTTGGAAAC-3', rev 5'-TTCTGGGTACATGGTGGTT-3'; *lag-2* for 5'-TGCGAAAACCTTTGTGATGC-3', rev 5'-TCGATGTTTGATTGGC-TGA-3'; *lin-39* for 5'-TGGGAGGTCCTCAATATCCA-3', rev 5'-CACCAC-TATGCTTTCTTG-3'.

Results

HPL-2 interacts with the LIN-13 zinc finger protein in vitro and in vivo

The *hpl-2* gene gives rise to two alternatively spliced transcripts, of which only one, *hpl-2a*, contains the

conserved full-length CD and CSD domains (Figs. 3A,B; Couteau et al., 2002). In all studies described here, *hpl-2* refers to the *hpl-2a* transcript only. We have previously shown that *hpl-2* encodes a ubiquitously expressed protein required for germline differentiation and vulval development (Couteau et al., 2002). Given that HP1 family proteins have been shown to interact with a number of nuclear factors (Eissenberg and Elgin, 2000; Li et al., 2002), the specificity of action of HPL-2 in germline and somatic development is likely to be due to interaction with specific proteins. To identify potential partners of HPL-2, a yeast two-hybrid screen was carried out. The bait used was composed of the full-length HPL-2 protein fused to the GAL-4 DNA binding domain (DB-HPL-2). Dimerization via the CSD has been shown to be required for HP1 to interact with at least a subset of proteins (Brasher et al., 2000; Thiru et al., 2004). To ask whether HPL-2 can dimerize, DB-HPL-2 and AD-HPL-2 fusion proteins were expressed in PJ69-4a and PJ69-4 α yeast strains respectively, and interaction was tested by mating. In the presence of both fusion proteins, *HIS3* and *ADE2* reporter genes were activated (Fig. 1A). This result was confirmed in an in vitro GST pulldown assay, using a purified recombinant N-terminally epitope tagged GST-HPL-2 and an in vitro translated ³⁵S-HPL-2 (Fig. 1B). We conclude that the self-dimerization property of HP1 family proteins is conserved in *C. elegans*. The DB-HPL-2 fusion protein was then used as a bait to screen a random primed *C. elegans* cDNA bank (kind gift from R. Barstead). Out of 4.8×10^7 transformants screened, we isolated one clone encoding a fragment of *lin-13*, a member of the LIN-35Rb class of genes involved in vulval development (Ferguson and Horvitz, 1989; Thomas et al., 2003). The LIN-13 protein is characterized by 24 zinc fingers of the C2-H2 class and a LXCXE Rb binding motif (Melendez and Greenwald, 2000). The clone isolated, in frame with the GAL-4-AD domain, contains residues 173 to 909 of the protein, including the LXCXE motif and the first five zinc fingers (Fig. 1C). Interaction was validated by re-transformation in strains PJ69-4a and PJ69-4 α , mating and testing reporter gene activity (Fig. 1A). To confirm the interaction, we performed binding studies using a GST-tagged HPL-2 protein and in vitro translated ³⁵S-LIN-13 protein in a GST-pulldown assay (Fig. 1B and supplementary material). ³⁵S-LIN-13 was retained on GST-HPL-2 but not GST-only resin, confirming the specificity of the two-hybrid interaction. We next asked if HPL-2 and LIN-13 also associate in vivo in *C. elegans*. To this end, we performed immunoprecipitation (IP) experiments from extracts expressing a functional LIN-13::GFP fusion protein using either GFP or HPL-2 specific antibodies, followed by Western blot analysis of the resulting immunocomplexes. As shown in Fig. 1D, we found that HPL-2 antibodies efficiently coimmunoprecipitated LIN-13::GFP from these extracts. Conversely, GFP antibodies directed against LIN-13::GFP were able to coimmunoprecipitate HPL-2. Neither HPL-2 nor LIN-13::GFP could be precipitated by non-specific antibodies. Therefore, the HPL-2/LIN-13 interaction observed in vitro is also found in vivo.

The CSD and Hinge region of HPL-2 are required for interaction with LIN-13 via a PLVPV HP1 consensus motif

For most known HP1-interacting proteins, association with HP1 involves the CSD (Lechner et al., 2000, 2005; Linder et al., 2001; Murzina et al., 1999; Nakayama et al., 2001; Vassallo and Tanese, 2002). To define the region of HPL-2 required for interaction with LIN-13, we performed binding studies with in vitro translated proteins deleted for the different domains of HPL-2. We tested CD alone, hinge (H) alone, H + CSD, and CSD alone (Figs. 2A and B). While the CSD alone was sufficient for interaction with LIN-13, this interaction was approximately 10-fold stronger when the hinge region was also included, as quantified by ImageQuant. Neither the hinge region nor the CD alone was able to interact with LIN-13. These results indicate that the CSD is essential for the interaction with LIN-13, and that amino acids present in the variable hinge region may contribute to this interaction. Since the CSD of HP1 proteins often interacts with a conserved pentapeptide motif PXVXL, we tested whether a PLVPV motif present in the N-terminal portion of LIN-13 included in the two-hybrid clone (Fig. 1C) is responsible for the interaction with HPL-2. We used site directed mutagenesis to change the conserved amino acids Val-442 and Val-444 to Asp (D) and Glu (E), respectively, to create AD-LIN-13^{PLDPE}. Substitution of these amino acids significantly reduced the interaction between HP1 and TAF_{II}130 (Vassallo and Tanese, 2002). After verifying the expression of the LIN-13^{PLDPE} mutant protein by Western blot analysis (data not shown), we tested its interaction with HPL-2 in the yeast two-hybrid system. As shown in Fig. 2C, the interaction of LIN-13 with HPL-2 was lost when the PLVPV sequence was mutated. Altogether, these results show that HPL-2 shares interaction properties with its homologues in other species.

Deletion of conserved residues within the CSD abolishes HPL-2 homodimerization but not interaction with LIN-13

Three *hpl-2* deletion alleles, *ok916*, *ok917*, and *tm1489*, have been independently isolated. *tm1489* comes from the Japanese National Bioresource Project, while *ok916* and *ok917* come from the *C. elegans* Knockout Consortium. We mapped the extent of the deletion in these alleles by sequencing the entire *hpl-2* coding sequence from homozygous mutant animals (see Supplementary material for experimental details). *ok916* is a 1739-bp deletion. RT-PCR analysis on total RNA from *ok916* mutant animals showed that this deletion results in the splicing of exon 3 to a cryptic splice donor site within exon 6, creating an open reading frame of 167 amino acids (aa) (Fig. 3A). *ok917* is a smaller deletion of 779 bp which joins exon 3 to exon 5 of *hpl-2b* and results in a frameshift. Sequence analysis showed that this mutation results in an open reading frame of 171 aa. The region deleted in *ok916* and *ok917* alleles includes conserved residues within the CSD domain (Figs. 3B, C). To study the potential effect of the loss of this region on the ability of

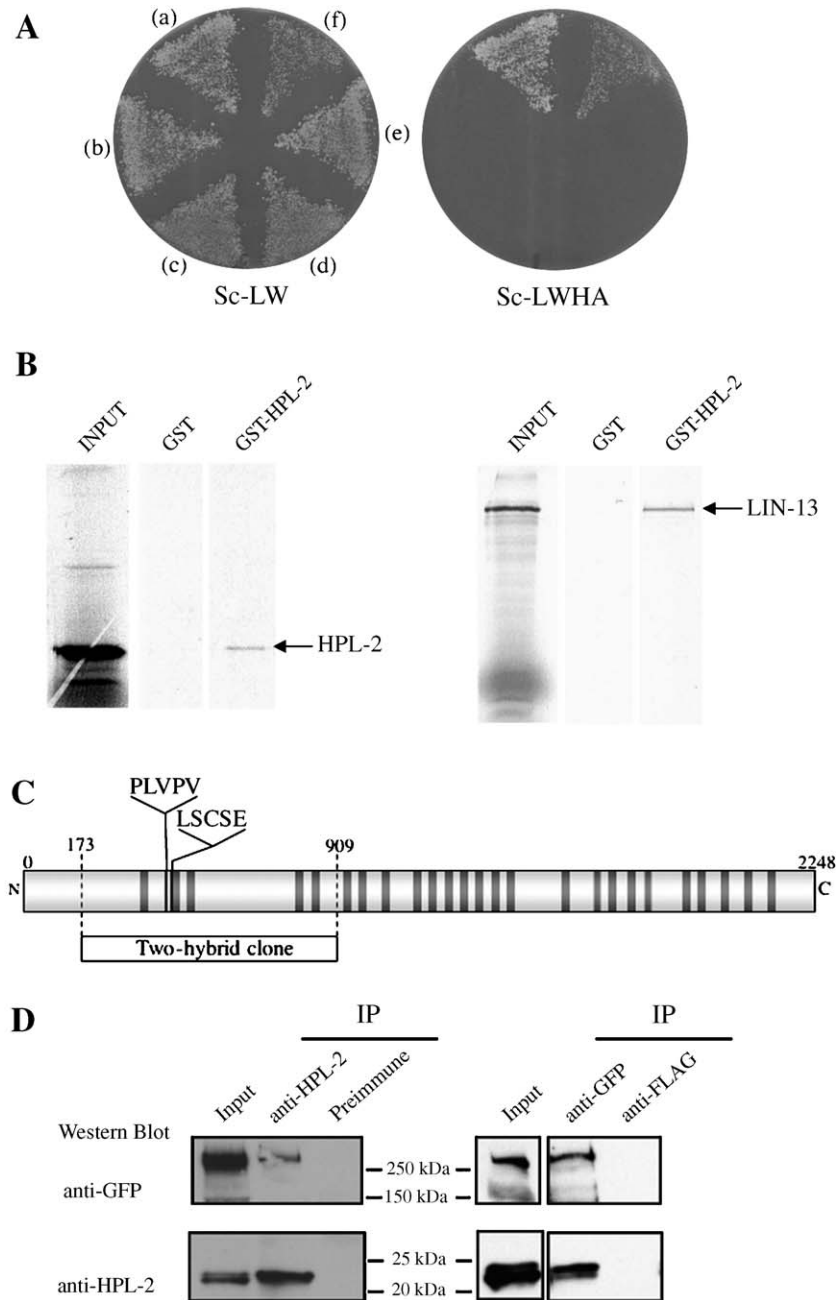


Fig. 1. HPL-2 self-dimerizes and interacts with LIN-13 in yeast two-hybrid and GST pulldown assays. (A) Two-hybrid assay. Left, selective media lacking leucine and tryptophan. Right, selective media lacking leucine, tryptophane, adenine and histidine supplemented with 1 mM 3-aminotriazole (3-AT). (a) DB-HPL-2 \times AD-LIN-13; (b) DB \times AD-LIN-13; (c) DB-HPL-2 \times AD; (d) DB \times AD; (e) DB \times AD-HPL-2; (f) DB-HPL-2 \times AD-HPL-2. (B) In vitro translated and labeled ^{35}S -HPL-2 (left panel) and ^{35}S -LIN-13 (right panel) were incubated with immobilized control GST or GST-HPL-2 (see Fig. 2). Bound interactors were eluted, resolved on SDS-PAGE and visualized by autoradiography. (C) Schematic representation of the LIN-13 protein. Solid bars represent zinc fingers. Position of both LSCSE Rb binding and PLVPV HP1 binding consensus motifs are indicated. The fragment corresponding to the cDNA clone recovered in the two-hybrid screen is indicated below the full-length sequence. (D) HPL-2 coimmunoprecipitates with LIN-13. Worm extracts derived from LIN-13::GFP transgenic animals were immunoprecipitated with anti-HPL-2 (left) or anti-GFP antibody (right) as indicated (IP), and the lysates were analyzed by Western blot. Input represents 1/50 of starting material. The third lane in each panel shows control IPs using either HPL-2 pre-immune sera, or anti-FLAG antibodies.

HPL-2 to dimerize and interact with LIN-13, we inserted a stop codon after nucleotide position 453 within the *hpl-2* sequence, corresponding to the 5' breakpoint of the *ok916* and *ok917* deletion alleles. This resulted in DB- and AD-tagged HPL-2 proteins with a partially deleted CSD. Following Western blot analysis to confirm expression of these truncated proteins in yeast (data not shown), two-hybrid

assays were performed to test their ability to homodimerize and interact with LIN-13. Surprisingly, we found that although the truncated protein was unable to homodimerize, it maintained the ability to interact with LIN-13 when assayed on SC minus histidine plus 1 mM 3-AT (Fig. 4) but not on higher concentrations of 3-AT or on SC minus adenine, suggesting that the interaction is nonetheless weaker

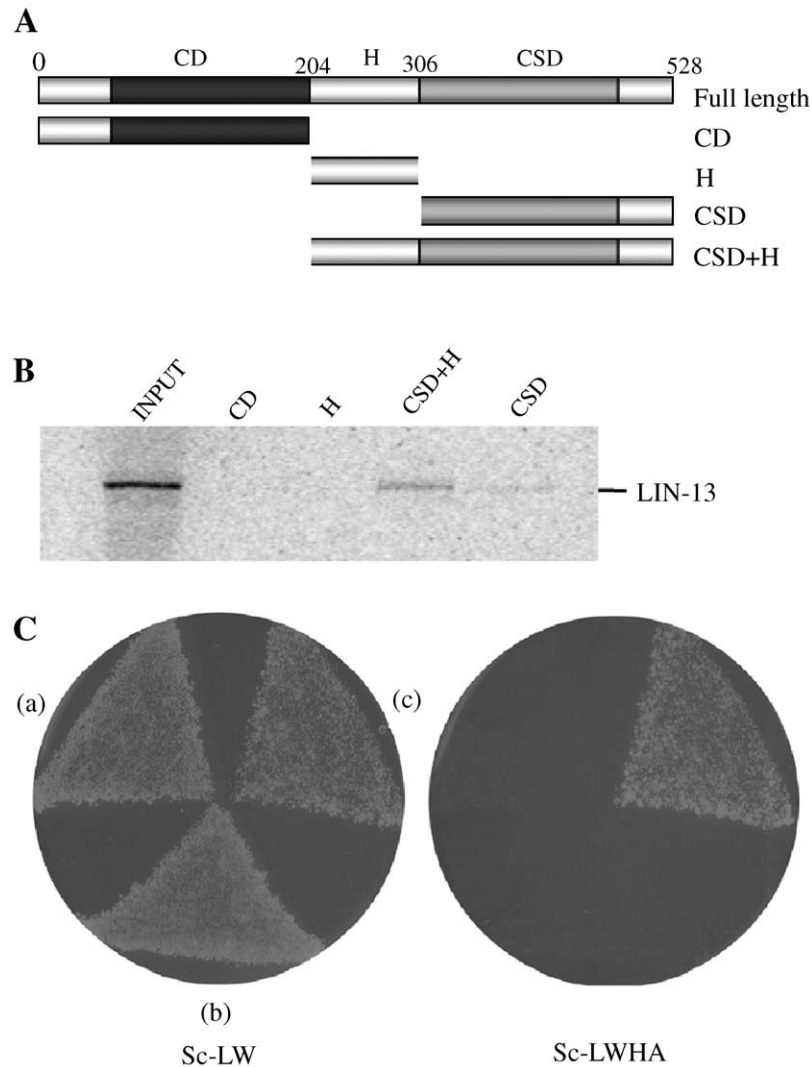


Fig. 2. Mapping of HPL-2 and LIN-13 interaction domains. (A) Schematic representation of full-length and truncated HPL-2 proteins tested by GST pulldown. CD, chromo domain; CSD, chromo shadow domain; H, hinge region. (B) GST-pulldown assays were performed with *in vitro* translated ^{35}S -LIN-13 incubated in a batch assay with immobilized GST or truncated proteins containing only the chromo domain (CD), hinge region (H), chromo shadow domain (CSD), or both chromo shadow and hinge regions (CSD + H). (C) The PLVPV motif present in LIN-13 is required for interaction with HPL-2. The full-length two-hybrid clone AD-LIN-13 and mutated AD-LIN-13^{PLDPE} were tested for interaction with DB-HPL-2 in a two-hybrid assay. Left, selective media lacking leu and trp. Right, selective media lacking leu, trp, his and ade. (a) DB-HPL-2 \times LIN-13^{PLDPE}; (b) DB \times LIN-13^{PLDPE}; (c) DB-HPL-2 \times LIN-13.

compared to full-length HPL-2. These results suggest that while the CSD residues missing in the *ok916* and *ok917* deletion alleles are essential for dimerization, they may not be absolutely required for the interaction of HPL-2 with the PLVPV motif of LIN-13. Sequencing of the *tm1489* allele confirmed that it is a deletion which starts 58 nucleotides upstream of the ATG and takes out the entire first and second exons, including sequences coding for the CD (Fig. 3A). This deletion is a clear molecular null allele, consistent with the observed phenotype, as described below.

hpl-2 and *lin-13* genetically interact with the *synMuv* pathway of vulval development

All three *hpl-2* mutant alleles show phenotypes similar to those we previously reported for *hpl-2* (RNAi) animals, including sterility, slow growth and an everted vulva (evl,

Table 1A; Couteau et al., 2002). However, the penetrance of these phenotypes appeared to be higher for the *ok917* and *tm1489* alleles, which at 25°C were also thin and scrawny and showed additional defects in vulva development. These data are consistent with the molecular analysis suggesting that *ok916* and perhaps *ok917* are not null alleles. The difference in the severity of phenotypes between *ok916* and *ok917* is likely to be due to differences in the residues added to the carboxyl terminus of the respective proteins.

In *C. elegans*, the vulva is derived from three of the six equivalent vulva precursor cells (VPCs), P(5–7).p (Sulston and Horvitz, 1977). The three other VPCs, P3.p, P4.p and P8.p normally adopt a cell fate giving rise to non-vulval cells. A conserved Ras-mediated signaling cascade is responsible for inducing the P(5–7).p cells to adopt a vulval fate (Aroian et al., 1990; Beitel et al., 1990) by overcoming inhibitory signals from two functionally redundant sets of genes, known as *synMuvA*

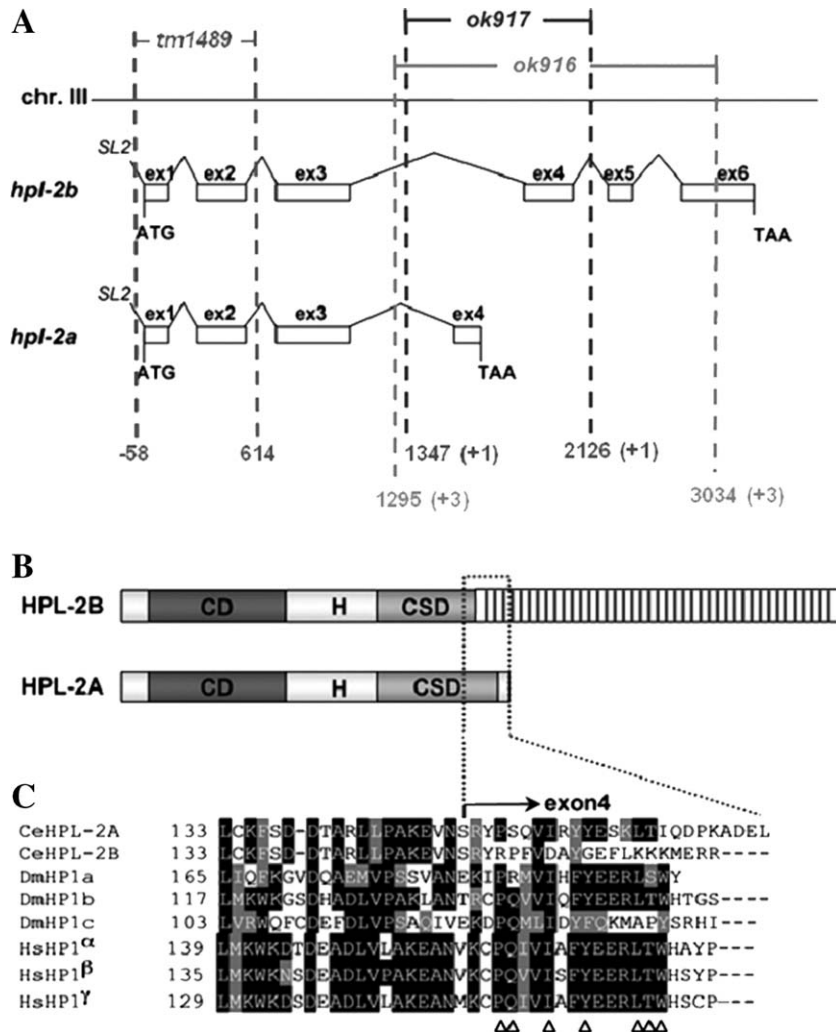


Fig. 3. Deletion mapping of the *ok916*, *ok917* and *tm1489* mutants. (A) Genomic structure of the *C. elegans hpl-2a* and *hpl-2b* gene products showing the region deleted in the three mutants (stippled lines). Deletion breakpoints are given with reference to the ATG start codon and bases of positional ambiguity are in the parentheses. (B) Schematic representation of the HPL-2A and HPL-2B proteins, showing the chromo domain (CD), chromo shadow domain (CSD), and hinge region (H). Dotted lines designate the highly conserved CSD region of HPL-2A aligned against other HP1 proteins in panel C. (C) Alignment of the amino acid sequence of the C-terminal end of the CSD from *C. elegans* HPL-2A (CeHPL-2A) and HPL-2B (CeHPL-2B), *D. melanogaster* HP1 isoforms (DmHP1a, -b, -c) and *H. sapiens* HP1 isoforms (HsHP1 α , - β , - γ). Black and gray shaded residues denote identical and conserved amino acids respectively, and amino acids essential for interaction are indicated by triangles.

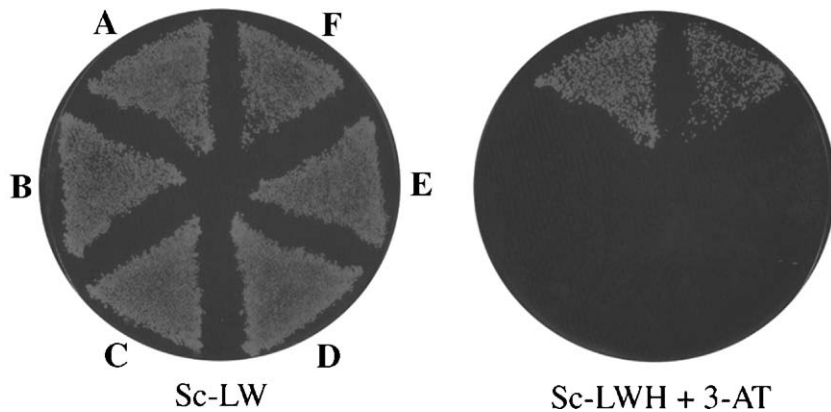


Fig. 4. HPL-2 Δ does not homodimerize but is able to interact with LIN-13. Left, selective media lacking leu and trp. Right, selective media lacking leu, trp, his with 1 mM 3-AT. (A) DB-HPL-2 Δ \times AD-LIN-13, (B) DB-HPL-2 Δ \times AD, (C) DB \times AD-HPL-2 Δ , (D) DB-HPL-2 Δ \times AD-HPL-2 Δ , (E) DB-HPL-2 Δ \times AD-HPL-2, (F) DB-HPL-2 \times AD-HPL-2.

Table 1
Phenotypic analysis of *hpl-2* deletion mutants and interaction with *lin-13*

A					
Genotype of progeny	Temperature (°C)	% Muv ^(a)	% Sterility	% evl	<i>n</i>
Wild type	25	0	0	0	>2000
<i>hpl-2(RNAi)</i>	25	<1 ^(b)	24–53 ^(b)	1–5 ^(b)	1852 ^(b)
<i>hpl-2(ok916)</i>	20	0	<1	0	995
<i>hpl-2(ok916)</i>	25	<1	98	1–10	376
<i>hpl-2(ok917)</i>	20	0	1–16	0	1770
<i>hpl-2(ok917)</i>	25	23	>99	45	669
<i>hpl-2(tm1489)</i>	20	0	14	0	341
<i>hpl-2(tm1489)</i>	25	34	100	72	1614
B					
synMuv allele combined with <i>hpl-2(tm1489)</i>	Class	% Muv at 20°C	% Muv at 25°C		
+	–	0 (<i>n</i> = 341)	34 (<i>n</i> = 1614)		
<i>lin-15A(RNAi)</i> ^(a)	A	100 (<i>n</i> = 72)	NA		
<i>lin-9(RNAi)</i> ^(b)	B	0 (<i>n</i> = 209)	77,2 ^(c) (<i>n</i> = 217)		
<i>lin-35(RNAi)</i> ^(b)	B	0 (<i>n</i> = 174)	73,4 ^(c) (<i>n</i> = 163)		
<i>lin-53(RNAi)</i> ^(b)	B	0 ^(d) (<i>n</i> = 124)	0 ^(d) (<i>n</i> = 98)		
C					
Genotype of progeny	Genotype of mother	Temperature (°C)	% Muv ^(a)	% Sterility	<i>n</i>
<i>lin-13(n388)</i>	<i>lin-13(n388)/+</i>	20	0	3–10	895
<i>lin-13(n388)</i>	<i>lin-13(n388)/+</i>	25	90	100	119
<i>hpl-2(tm1489)</i>	<i>hpl-2(tm1489)/+</i>	25	0	10	212
<i>lin-13(n388) hpl-2(tm1489)</i>	<i>lin-13(n388) hpl-2(tm1489)/+</i>	20	0	95	128
<i>lin-13(n388) hpl-2(tm1489)</i>	<i>lin-13(n388) hpl-2(tm1489)/+</i>	25	96	100	127
<i>lin-13(n388)</i>	<i>lin-13(n388)</i>	20	0	100	>500
<i>lin-13(n388) hpl-2(tm1489)</i>	<i>lin-13(n388) hpl-2(tm1489)</i>	20	38	100	211 ^(b)

(A) *hpl-2* mutant phenotypes. Animals were derived from homozygous mothers grown at 20°C, and when indicated shifted at 25°C as early L4. Ranges indicate variations between experiments. ^(a)Animals were scored as Muv if they showed at least one ectopic pseudovulva under a dissecting microscope. ^(b) Taken from Couteau et al. (2002). (B) Genetic interaction between *hpl-2(tm1489)* mutants and synMuv genes. synMuvA or B genes were inactivated in *hpl-2(tm1489)* animals by RNAi by either injection ^(a) or feeding ^(b). Animals were scored as Muv as in (A). When specified, Muv phenotypes were scored among escapers of the larval arrest phenotype ^(c), or among escapers of the embryonic lethality ^(d) in early broods.

(C) Genetic interaction between *hpl-2* and *lin-13*. Heterozygous parents were grown at 20°C or 25°C as indicated. ^(a) Animals were scored as Muv as in (A). ^(b) *hpl-2 lin-13* progeny from fertile *hpl-2 lin-13* escapers.

and B (Ferguson and Horvitz, 1989). When any two redundant signaling systems are disabled, P3.p, P4.p and P8.p cells adopt vulval fates and produce a Muv phenotype. Given that RNAi experiments suggested a role for *hpl-2* in the synMuvB pathway (Couteau et al., 2002), we tested the *hpl-2* mutant alleles for a Muv phenotype in either synMuvA or B mutant backgrounds.

We found that for all three *hpl-2* deletion alleles, RNAi inactivation of class A, but not class B synMuv genes results in a highly penetrant Muv phenotype at 20°C (Table 1B and data not shown). This phenotype is dependent on a functional RTK/Ras/Map kinase pathway (Couteau et al., 2002 and data not shown). At 25°C, however, *ok917* and *tm1489* mutations alone result in a Muv phenotype (Table 1A). Furthermore, at 25°C inactivation of synMuvA or B genes in an *hpl-2* mutant context results in severe developmental defects, including larval lethality. Altogether, these results suggest that although at 20°C *hpl-2* behaves as synMuvB genes, at 25°C it has additional functions redundant with both synMuvA and B genes.

Like *hpl-2*, *lin-13* strictly behaves as a synMuvB gene at 15°C and 20°C but shows a Muv phenotype at 25°C (Table 1C; Ferguson and Horvitz, 1989; Melendez and Greenwald, 2000; Thomas et al., 2003). Surprisingly, we found that at 20°C, *hpl-2*

lin-13 double mutant animals without maternal contribution also showed a Muv phenotype (38%, *n* = 211, see Supplementary material for strain construction). In addition, in the presence of maternal contribution of both gene products, these animals also showed a synergistic increase in sterility. Since both the *lin-13* and *hpl-2* alleles used in these experiments are nulls, these results suggest that although both genes participate in vulval development by acting in the same complex with at least some of the synMuvB genes, they may have additional, redundant functions in both vulval and germline development.

The fact that at 25°C *hpl-2* mutants show an interaction with both synMuvA and B mutants raised the possibility that *hpl-2* may belong to the recently described synMuvC group of genes (Ceol and Horvitz, 2004). However, while synMuvC mutants alone or in combination with synMuvB mutants mostly affect the specification of P8.p, the Muv phenotype associated with *hpl-2* single mutants at 25°C concerns P3.p, P4.p and P8.p cells, which were induced respectively in 44%, 78% and 56% of animals showing a Muv phenotype (*n* = 23). Furthermore, we found that inactivation of the synMuvC gene *trr-1/TRRAP* in an *hpl-2* mutant background resulted in synthetic lethality. While *trr-1(RNAi)* feeding on wild-type worms did not cause any embryonic lethality at either 20°C or 25°C (*n* = 66 and *n* = 191,

respectively), *trr-1*(RNAi) feeding on *hpl-2*(tm1489) worms resulted in 30% ($n = 212$) embryonic lethality at 20°C and 60% ($n = 202$) embryonic lethality at 25°C. In both cases, 100% of the remaining progeny arrested development as early larvae. *trr-1*(RNAi) was also found to result in embryonic lethality in combination with several other synMuvB genes tested (Ceol and Horvitz, 2004). Although we considered the possibility that the synergistic effect, we observe might be due to the enhanced response to dsRNA recently reported for several synMuvB mutants (Wang et al., 2005), we think this unlikely as the synMuvB mutations found to synergize with *trr-1*(RNAi) by Ceol and Horvitz (2004) include ones shown to have an enhanced RNAi response (*lin-35*, *dpl-1*), as well as ones that do not (*lin-36*, *lin-37*). Altogether, these results suggest that *hpl-2* and the synMuvC genes act in distinct pathways in vulval development, while for viability *trr-1* may function redundantly with *hpl-2*.

HPL-2 localization in nuclear foci depends on LIN-13

We previously showed that an HPL-2::GFP fusion protein is ubiquitously expressed in most, if not all nuclei throughout embryonic and larval development and into adulthood, with a signal concentrated in a limited number of nuclear foci in early embryos (Couteau et al., 2002). Interestingly, a LIN-13::GFP fusion protein shows very similar nuclear foci in embryos (Melendez and Greenwald, 2000), suggesting that both HPL-2 and LIN-13 may be enriched in particular nuclear subdomains. To test whether the two proteins colocalize in at least some of these nuclear foci, we constructed a transgenic strain coexpressing both HPL-2::RFP and LIN-13::GFP fusion proteins. In early stage live embryos, we observed an overlap of most of the larger LIN-13 and HPL-2 nuclear foci (Figs. 5A–C). These results are consistent with HPL-2 and LIN-13 interacting at a subset of specific chromosomal sites. We next asked whether there is interdependence in the localization of HPL-2 and LIN-13. To this end, we performed *lin-13*(RNAi) on HPL-2::GFP strain and introduced the LIN-13::GFP construct in the *hpl-2* (tm1489) mutant strain. In wild-type embryos, *hpl-2*::GFP is concentrated in a median number of 15.4 foci per nucleus (Fig. 6). Strikingly, these HPL-2 foci were completely lost in *lin-13* (RNAi) animals (Figs. 5D–G, 6). By contrast, LIN-13 nuclear foci were unaltered in the absence of *hpl-2* (Figs. 5L–M).

We next tested whether RNAi of other synMuvB genes, including *lin-9*, *lin-35*, *hda-1*, *let-418* and *mep-1* might also effect HPL-2 localization (Figs. 5I–K and Fig. 6). While *lin-9*, *lin-35*, *let-418* and *mep-1* had no significant effect on the number of HPL-2 nuclear foci (one-way ANOVA test, followed by

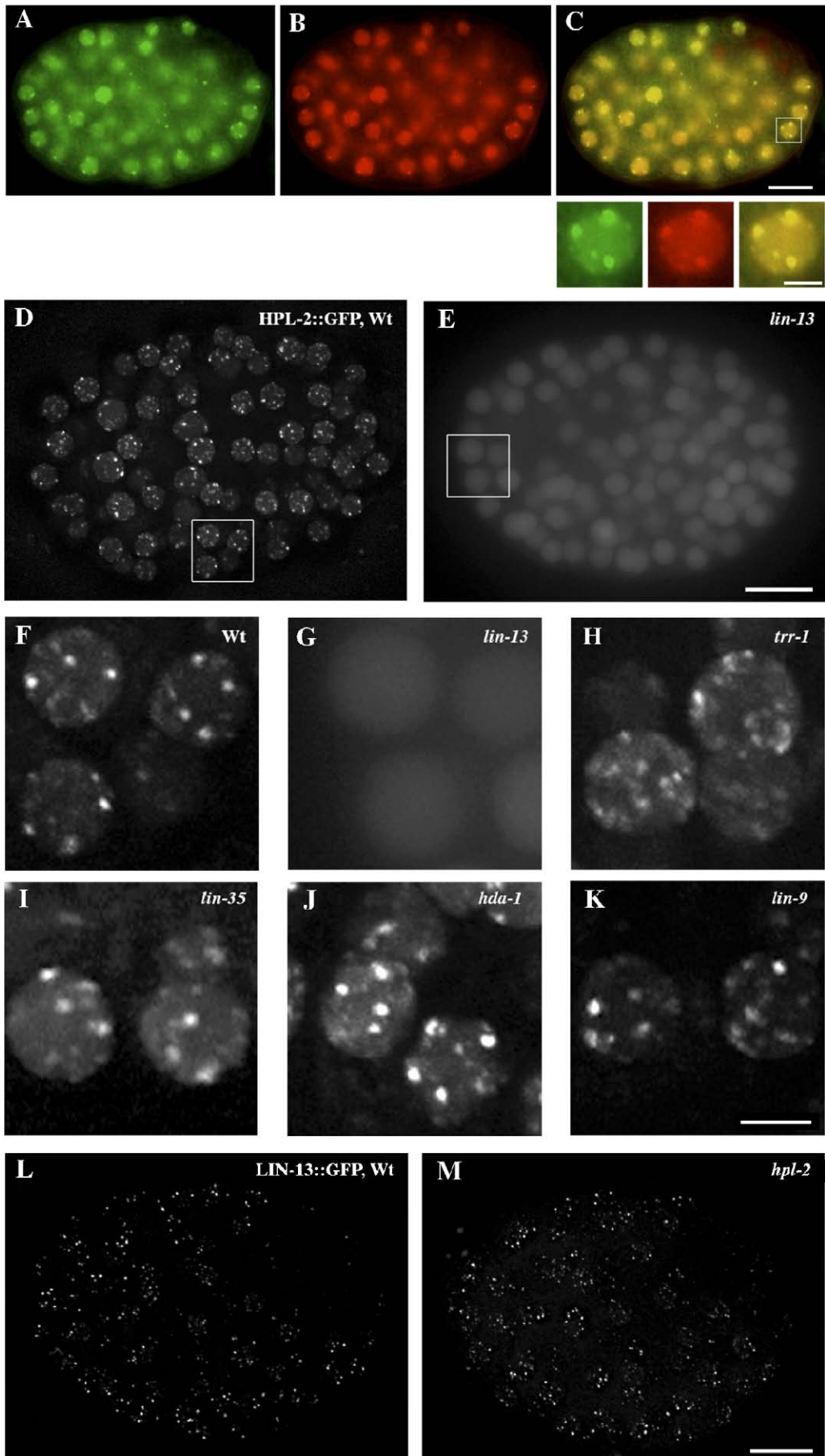
Tukey Honest Significant Differences; $P < 0.001$), in *hda-1* (RNAi) embryos the median number of foci per nucleus was found to increase to 18.0 (Fig. 6). We also tested the synMuvA gene *lin-15A* but were unable to obtain a reliable count of the number of foci per nucleus due to defects in nuclear morphology in a significant fraction of the embryos observed. Interestingly, inactivation of the synMuvC genes *trr-1* and *mys-1* had a pronounced effect on the median number of HPL-2 foci per nucleus, which was found to increase to 20.0 and 18.4 respectively (Fig. 5H and Fig. 6). Altogether, these results suggest that while LIN-13 alone may be sufficient for recruiting HPL-2 in nuclear foci, other synMuv genes, including the class B gene *hda-1*, and the class C genes *trr-1* and *mys-1*, may also either directly or indirectly influence this recruitment to a subset of chromosomal sites.

HPL1 specifically recognizes the H3 N-terminal tails when di- and tri-methylated on lysine 9 (MeK9H3) (Bannister et al., 2001; Jacobs et al., 2001; Lachner et al., 2001; Nakayama et al., 2001; Nielsen et al., 2002). To ask whether H3-K9 methylation might also play a role in the recruitment of HPL-2, we stained fixed samples with tri-methyl K9 antibodies in combination with anti-GFP antibodies to detect the HPL-2::GFP fusion protein. As shown in Fig. 7, although a partial overlap between the two signals can be detected in some cases, the majority of the large HPL-2 foci do not colocalize with tri-methyl K9 staining. Similar results were obtained with di-methyl K9 antibodies (data not shown). These results suggest that the large HPL-2 foci that we observe do not correspond to chromosomal regions enriched in H3-K9 methylation, although at other chromosomal sites HPL-2 and H3-K9 methylation may overlap.

lin-13 and hpl-2 regulate the expression of specific genes

To gain insight into the molecular mechanism responsible for the *hpl-2* and *lin-13* phenotypes, we sought to identify potential targets of these two genes using various cell type-specific GFP reporter transgenes. Several synMuv genes have been shown to regulate the *lin-39Hox* gene in VPCs (Chen and Han, 2001). To test whether *lin-13* and *hpl-2* have a similar function, we used an integrated *lin-39*::GFP reporter transgene normally weakly expressed in a subset of VPCs and more strongly in nerve cord neurons (Fig. 8A). In *hpl-2* and *lin-13* mutants, we observed an increased expression of the *lin-39* reporter in neuronal cells as well as additional unidentified cells in the mid-body region (Figs. 8B, C). Although we were unable to specifically quantify GFP expression in VPCs, the relevant targets for vulval cell fate specification, these results suggest that *hpl-2* and *lin-13* may play a more general role in the regulation of *lin-39* expression.

Fig. 5. HPL-2 localization in nuclear foci depends on LIN-13. (A–C) Localization of HPL-2 and LIN-13 in a live 64-cell stage embryo. (A) LIN-13::GFP (B) HPL-2::RFP (C) Merge. Images correspond to one optical section, not submitted to deconvolution. Scale bar represents 10 μ m. Inserts in panel C show an enlargement of the boxed nucleus. Scale bar represents 2.5 μ m. (D–G) HPL-2::GFP foci disappear in *lin-13*(RNAi)-treated animals. (D) HPL-2::GFP expression in a live wild-type embryo (74-cell stage). (E) HPL-2::GFP expression in a live *lin-13*(RNAi) embryo (72-cell stage). Scale bar represents 10 μ m. (F–G) Images show an enlargement of boxed nuclei visible in panels D and E, respectively. (H–K) Enlargements of live embryos expressing *hpl-2*::GFP in different RNAi backgrounds, *trr-1* (H), *lin-35* (I), *lin-15B* (J), *lin-9* (K). (L–M) LIN-13::GFP foci are not affected in *hpl-2*(tm1489) animals. LIN-13::GFP expression is shown in a live wild-type embryo (L) or in a live *hpl-2*(tm1489) mutant embryo (M). Images shown in panels D–K correspond to maximum intensity projection of deconvolved sections and are display with the same dynamic for comparison purposes, except for *lin-13* images (E, G), whose dynamics were increased by a factor of 4. Images shown in panels L–M correspond to maximum intensity projection of deconvolved sections and are display with the same dynamic for comparison purposes Scale bar represents 2.5 μ m (F–K).



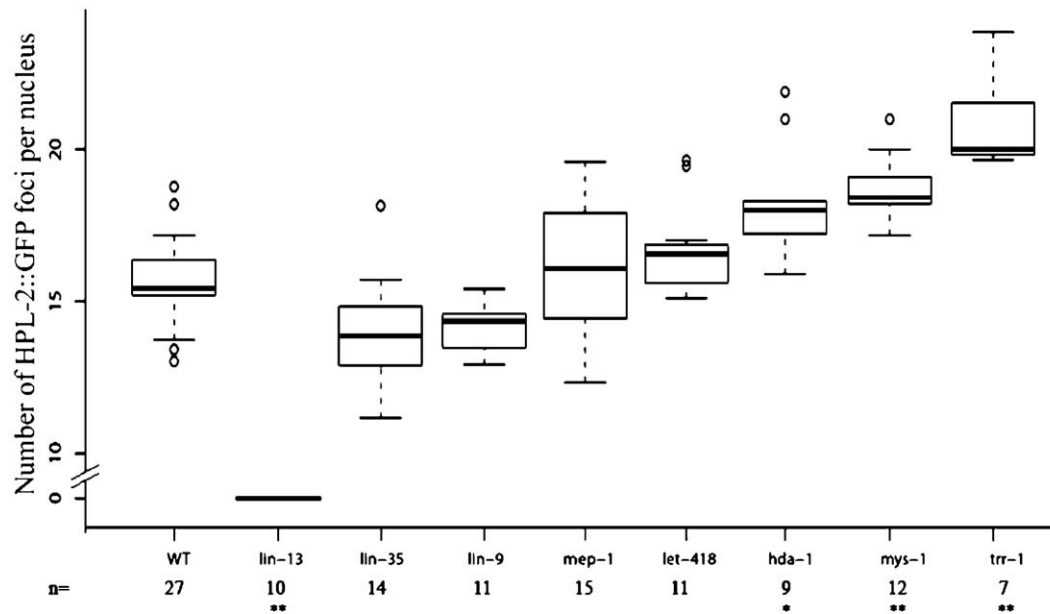


Fig. 6. Quantitation of HPL-2::GFP foci in wild-type and mutant conditions. A box plot representation of the number of HPL-2::GFP foci in different synMuv RNAi backgrounds is shown. The x axis indicates genotypes; the y axis indicates the number of HPL-2::GFP foci observed per nucleus. The center horizontal line of each box indicates the median value; the box to and bottom indicate the first and third quartile values; the line above and below the boxes extend to the entire range of measurements. *n* Represents the number of embryos analyzed for each genotype. **P* < 0.001; ***P* < 0.0001, one-way analysis of variance and Turkey multiple comparison of mean differences compared to WT.

We also found that a *lag-2::GFP* reporter was widely derepressed in both mutant backgrounds, as previously shown for HDA-1 and more recently other synMuv genes (Dufourcq et al., 2002; Poulin et al., 2005). As shown in Fig. 8D, in wild-type animals expression of *lag-2::GFP* is restricted to the distal tip cell of the gonad, the ventral nerve cord and a few cells of the vulva. In *hpl-2* and *lin-13* animals, *lag-2::GFP* expression was widely derepressed, notably in cells of the pharynx, hypodermis and intestine (Figs. 8E, F). The effect on *lag-2* and *lin-39* expression is unlikely to be due to a general effect of the *hpl-2* and *lin-13* mutations on transgene expression as we did not notice any effect on the expression of several other transgenes in the soma, either in an extrachromosomal or integrated context (data not show). Furthermore, quantitative real-time PCR analysis using RNA derived from a mixed stage population of worms revealed a threefold increase in *lin-39* expression and a two and a half-fold increase in *lag-2* expression in *hpl-2* animals compared to wild-type (Fig. 8G). Altogether, these results are consistent with *hpl-2* and *lin-13*

playing a role in either directly or indirectly repressing the expression of specific genes.

Discussion

HPL-2 interaction with *LIN-13* relies on conserved domains

HP1 family proteins are essential components of constitutive heterochromatin in both yeast and *Drosophila*. More recent evidence from mammals suggests a broader role for HP1 family proteins in the epigenetic regulation of gene expression. Several examples of gene-specific recruitment of HP1 via its association with transcriptional regulators that bind specific DNA sequences have been reported (Ayyanathan et al., 2003; Nielsen et al., 2001; Ogawa et al., 2002). In vitro, the association of TIF1 with HP1 has been shown to be required for progression through differentiation (Cammass et al., 2004), while Rb has been found to be associated with the recruitment of HP1 to the cyclin E promoter (Nielsen et al., 2001). An interaction with the

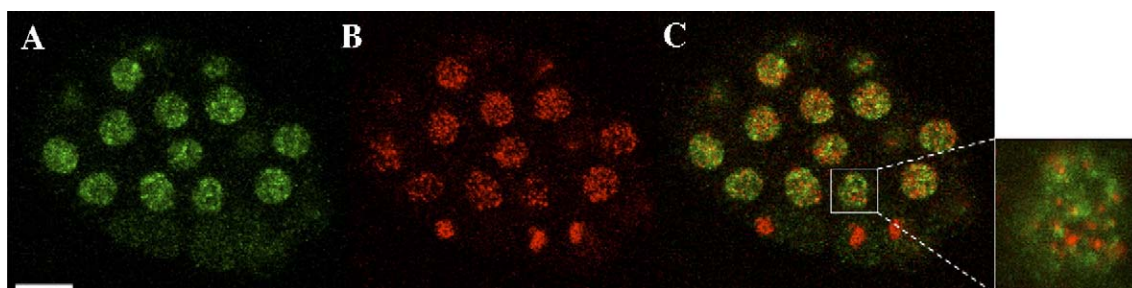


Fig. 7. HPL-2::GFP foci are not enriched in H3K9Me3. (A) HPL-2::GFP (B) H3K9Me3 (C) merge. Insert shows an enlargement of the boxed in nucleus. Scale bar represents 10 μ m.

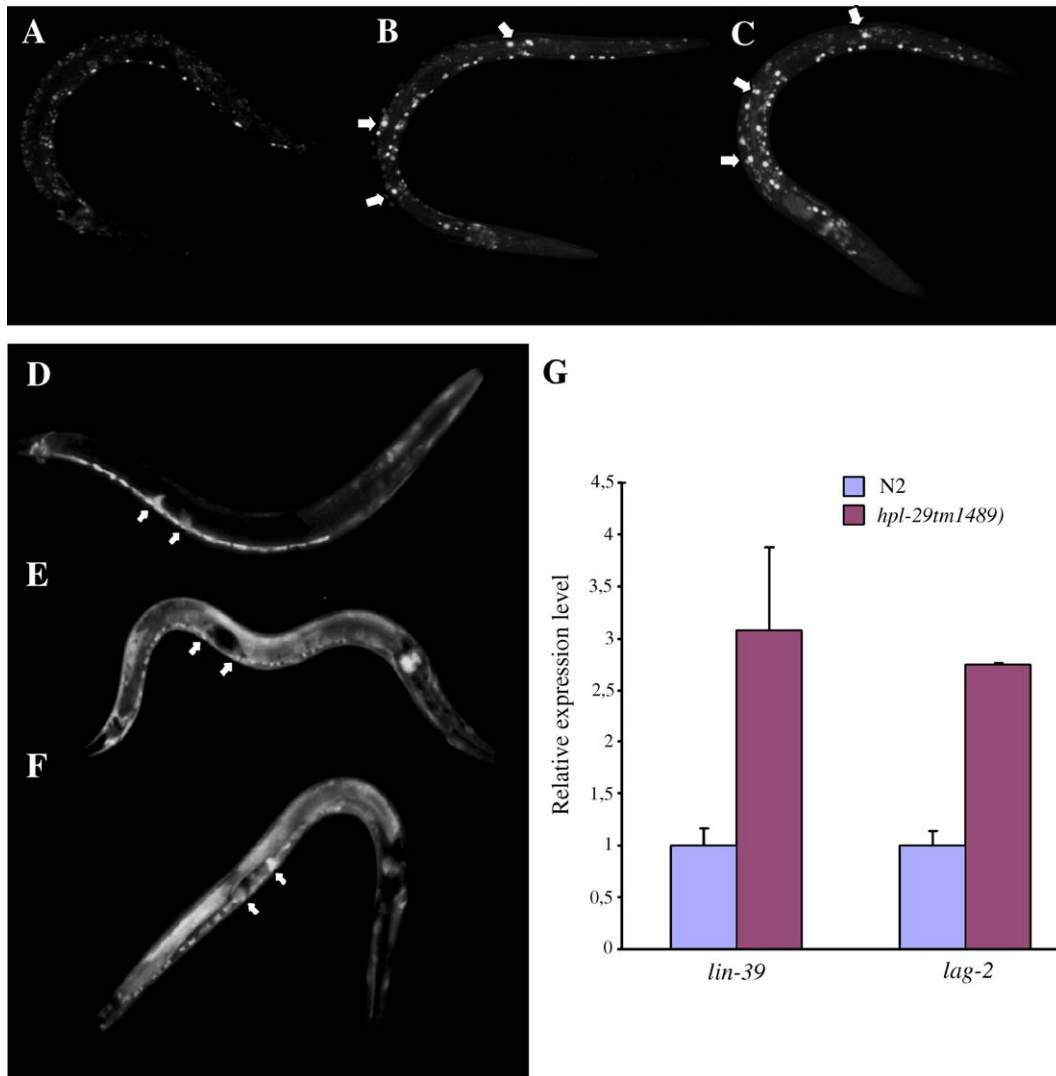


Fig. 8. HPL-2 and LIN-13 influence *lin-39::GFP* and *lag-2::GFP* gene expression. (A–C) Expression of *lin-39::GFP* in late L2 larvae of strain qIs56 at 25°C is shown in green. Anterior end is up, posterior down. White arrows point to examples of cells in which ectopic GFP expression is observed. (a) *lin-39::GFP* expression in a wild-type animal; (b) *lin-39::GFP* expression in a *hpl-2(tm1489)* animal; (c) *lin-39::GFP* in a *lin-13(RNAi)* animal. (D–F) Expression of *lag-2::GFP* in L2 larvae at 25°C is shown in green. White arrows indicate distal tip cells (DTC). (d) *lag-2::GFP* expression in a wild-type animal; (e) *lag-2::GFP* expression in a *hpl-2(tm1489)* mutant background; (f) *lag-2::GFP* expression in a *lin-13(RNAi)* animal. (G) Endogenous *lag-2* and *lin-39* RNA levels were quantified in wild-type and *hpl-2(tm1489)* worms by real-time quantitative RT-PCR. *lag-2* and *lin-39* expression levels were arbitrarily set to 1 in the wild-type background. Error bars, SEM.

E2F-6 complex has also been shown to mediate recruitment of HP1 to the promoter of E2F and myc-responsive genes (Ogawa et al., 2002). Nonetheless, the role played by HP1 proteins in specific developmental context remains poorly understood. In *C. elegans*, the synMuvB pathway of vulval development includes homologues of the recently described RB containing complexes Myb-MuvB or dREAM (Korenjak et al., 2004; Lewis et al., 2004). Here, we have shown that HPL-2 physically interacts with the LIN-13 zinc finger protein, another component of the Rb-related synMuvB pathway, both in vitro and in vivo, and that this interaction is required for the recruitment of HPL-2 in nuclear foci. Our results suggest that HPL-2 shares interaction properties with its homologues in other species. Most notably, interaction with LIN-13 involves both CSD and hinge regions, and is mediated by a PLVPV motif in the N-terminus of LIN-13.

Unique and redundant functions of *hpl-2* and *lin-13* in development

We find that *hpl-2* and *lin-13* share several properties that distinguish them from classical synMuvB genes. By definition, synMuvB mutants only result in a Muv phenotype in combination with mutations in the synMuvA pathway, and do not genetically interact (Ferguson and Horvitz, 1989). By contrast, at 25°C mutations in *hpl-2* and *lin-13* alone give rise to a significant percentage of Muv animals. In addition, at 20°C *hpl-2* and *lin-13* double mutants show a Muv phenotype and a synergistic increase in sterility. Altogether, these results suggests that although HPL-2 and LIN-13 may participate in vulval development by acting in the same complex with at least some of the synMuvB proteins, they are likely to have additional, redundant functions in both vulval and germline

development. The exquisite temperature dependence of the phenotypes observed for both *lin-13* and *hpl-2* has already been noted for other synMuv genes (Ferguson and Horvitz, 1989; Thomas et al., 2003). Elevated temperature conditions have been shown to be associated with defects in heterochromatin assembly in different systems (Allshire et al., 1995; Ayoub et al., 1999; Spofford, 1976), consistent with the idea that at least a subset of synMuv genes including *hpl-2* and *lin-13* act in chromatin-related pathways. The Muv phenotype observed at 25°C could be attributed to the participation of *hpl-2* and *lin-13* to both synMuvA and B pathways, or to yet another pathway at this temperature. Ceol and Horvitz recently described a third class of synMuv genes, called synMuvC, that encode homologues of the Tip60/NuA4 histone acetyltransferase complex and act redundantly with both class A and B genes (Ceol and Horvitz, 2001). Our data suggest that in vulval cell fate specification, *hpl-2* acts independently of synMuvC genes, consistent with multiple chromatin modifying proteins being implicated in this specific developmental pathway.

The observation that depletion of both maternal and zygotic activity at 25°C results in larval arrest for *lin-13*, and adult sterility for *hpl-2*, is consistent with LIN-13 and HPL-2 having additional, independent functions in larval development. Consistently, HP1 family proteins are known to interact specifically with a number of different nuclear proteins and in addition to LIN-13 we have isolated a number of other potential HPL-2 partners (M. Karali and F. Palladino, unpublished). In the context of the dynamic structure of chromatin, only a subset of HP1 interactions are likely to take place in a given cell type at a specific stage of development.

lin-13 and hpl-2 may regulate the expression of specific genes

Our data suggest that *lin-13* and *hpl-2* may play a general role in regulating the expression of at least two genes, the *lin-39*Hox and the *lag-2* Notch ligand genes. Both *lag-2::GFP* and *lin-39::GFP* reporters were widely derepressed in both *hpl-2* and *lin-13* mutant backgrounds. Interestingly, the *C. elegans* Polycomb group proteins MES-2, MES-3 and MES-6, involved in the chromatin based control of gene expression in the germline, have also been shown to repress Hox expression in the soma (Ross and Zarkower, 2003), while *lag-2* expression has previously been shown to be negatively regulated by the histone deacetylase *hda-1* (Dufourcq et al., 2002) and more recently other synMuvB and C genes (Poulin et al., 2005). During vulval development, *lag-2* acts in a LIN-12/Notch signaling pathway which prevents certain VPCs from adopting the primary vulval cell fate (Chen and Greenwald, 2004; Sternberg, 1988). The global ectopic expression of the *lag-2::GFP* reporter we observe in *hpl-2* and *lin-13* mutant animals suggests that *lag-2* expression may be under control of *lin-13* and *hpl-2*. *lin-12* gain of function alleles (Greenwald et al., 1983) and ectopically expressed mutant forms of LAG-2 (Henderson et al., 1997) result in multivulval phenotypes. In principle, derepression of LAG-2 could therefore result in the same phenotype and contribute to the Muv phenotype observed in single *hda-1*, *lin-13* and *hpl-2* mutant strains (Dufourcq et al.,

2002, our data). We note however that, in contrast to *lin-12* gain of function alleles which cause a Muv phenotype because all six Pn.p cells adopt 2° vulval cell fates (Greenwald and Seydoux, 1990), in *hpl-2* and *lin-13* single mutants ectopically induced VPCs adopt 1° and 2° cell fate, as shown for other synMuv (data not shown and Sternberg, 1988). Regardless of the precise mechanism, our results are consistent with HPL-2 and LIN-13, together with other synMuv proteins, regulating gene expression either directly or indirectly in multiple developmental pathways.

A function for LIN-13 in recruiting HPL-2 to chromatin

Consistent with an interaction between HPL-2 and LIN-13, we have shown that the foci observed in embryos with HPL-2::RFP and LIN-13::GFP fusion proteins overlap. Furthermore, HPL-2 localization in these foci is strictly dependent on LIN-13, while LIN-13 distribution does not seem to be affected in the absence of HPL-2. Altogether, these results strongly suggest that LIN-13 directly recruits HPL-2 to a limited number of target loci. Nonetheless, our localization studies show that other synMuv genes may also influence HPL-2 localization. Most notably, we found that inactivation of synMuvC genes and to a lesser extent *hda-1*/HDAC, resulted in a significant increase in the number of HPL-2 nuclear foci. The synMuvC genes encode homologues of the TIP60/NuA4 histone acetylase complex, which could act either in transcriptional repression or activation (Ceol and Horvitz, 2004), while class I histone deacetylase such as HDA-1 are associated with repression. One interpretation of the effect of inactivation of *trr-1*, *mys-1*, and to a lesser extent *hda-1*, on HPL-2 distribution is that the dynamic acetylation/deacetylation equilibrium of specific chromosomal regions is perturbed, leading to recruitment of HPL-2 to ectopic sites. One possible consequence of this ectopic recruitment may be to reduce the amount of HPL-2 available for repression at target genes. We note that while LIN-13 distribution was not affected by inactivation of most of the synMuvB genes tested in this study (data not shown), inactivation of *trr-1* had an effect on LIN-13 distribution similar to that observed for HPL-2, reinforcing the idea that chromatin architecturation may be perturbed in a synMuvC mutant context.

Although HP1 proteins have been shown to bind chromatin by specifically recognizing histone H3 N-terminal tails methylated on lysine 9 (MeK9H3), several recent reports suggest that HP1 can also be found on chromatin independently of MeK9H3 (Cowell et al., 2002; Greil et al., 2003; Li et al., 2003), indicating the existence of more than one mechanism of HP1 recruitment. Our data suggest that LIN-13 may provide one such mechanism. Nonetheless, MeK9H3 may target HPL-2 to other chromosomal regions, as we were able to observe some overlap in HPL-2 and MeK9H3 localization, and HPL-2 does show an in vitro binding preference for peptides methylated on lysine 9 (data not shown). Furthermore, LIN-13 cannot be the sole mechanism for targeting HPL-2 because while in larva and adults *hpl-2* expression persists in most if not all cell types, including VPCs and hypodermal cells (Cousteau et al., 2002), LIN-13 expression is

very low and limited to a few cell types including hypodermal cells but not VPCs (Melendez and Greenwald, 2000). Interestingly, recent data suggest that for LIN-35Rb, the relevant transcription targets for vulval cell fate specification are likely to be in the hypodermal syncytium (Myers and Greenwald, 2005). If HPL-2 and LIN-13 interact as a single complex in vulval cell fate specification, they are also likely to act in hypodermal cells, where both proteins are expressed. Altogether, our data suggest that LIN-13, HPL-2 and other synMuv proteins including HDA-1, LIN-35Rb, and LIN-9 may be found either in the same or in distinct repressor complexes depending on the specific developmental pathway. In *Drosophila*, the presence of at least two distinct RB complexes, termed dREAM and myb-MuvB, has recently been described (Korenjak et al., 2004; Lewis et al., 2004). Interestingly, while both complexes were found to contain homologues of synMuvB gene products, they differed in the presence of individual subunits. In a more general way, we suggest that in *C. elegans* the LIN-13/HPL-2 complex may act as a chromatin scaffold that, in turn, coordinates the activities of large macromolecular complexes that modify chromatin structure to silence gene expression, including the synMuvB complex. In this context, LIN-13 may fulfill a function similar to the mammalian KAP1-KRAB repressor system, which directs binding and deposition of HP1 to silence gene expression (Abrink et al., 2001; Lechner et al., 2000; Peng et al., 2000; Schultz et al., 2002).

It has been recently shown that members of the *C. elegans* Rb pathway, including the synMuvB genes *lin-35Rb*, *dpl-1DP* and *lin-9*, negatively regulate RNAi, presumably through the repression of a subset of RNAi genes in the soma (Wang et al., 2005). Of particular interest, *hpl-2* and *lin-13*, but not other synMuv genes, were found to have a similar function. However, despite the fact that both HPL-2 and LIN-13 proteins contain a putative Rb binding motif, so far we have been unable to detect a direct interaction between LIN-35Rb and either HPL-2 or LIN-13. Further analysis is required to gain better understanding of the link between LIN-35Rb, LIN-13, HPL-2 and other synMuv class genes in vulval and other developmental pathways. These studies should contribute to an understanding of how HP1 and other chromatin-associated proteins may be adapted to specific pathways of development in higher eukaryotes.

Acknowledgments

We are grateful to M. Labouesse for critical reading of the manuscript, J.B. Sibarita for providing expertise with deconvolution, G. Yvert for providing expertise with statistical analyses, and the Microscopy platform of the IFR128. Thanks to Y. Kohara for cDNA clones, K. Giesler and E. Goillot for yeast strains, the *C. elegans* Knockout Consortium and the National BioResource Project for *hpl-2* alleles. Some *C. elegans* strains were obtained from the *Caenorhabditis* Genetic Center, which is supported by the National Center for Research. This work was supported by the CNRS and the Association pour la Recherche sur le Cancer (ARC). V. Coustham was supported by the Ministère de la Recherche and the ARC. K. Monier was supported by the Federation pour la Recherche Medicale.

References

- Abrink, M., Ortiz, J.A., Mark, C., Sanchez, C., Looman, C., Hellman, L., Chambon, P., Losson, R., 2001. Conserved interaction between distinct Kruppel-associated box domains and the transcriptional intermediary factor 1 beta. *Proc. Natl. Acad. Sci. U. S. A.* 98, 1422–1426.
- Allshire, R.C., Nimmo, E.R., Ekwall, K., Javerzat, J.P., Cranston, G., 1995. Mutations derepressing silent centromeric domains in fission yeast disrupt chromosome segregation. *Genes Dev.* 9, 218–233.
- Aroian, R.V., Koga, M., Mendel, J.E., Ohshima, Y., Sternberg, P.W., 1990. The *let-23* gene necessary for *Caenorhabditis elegans* vulval induction encodes a tyrosine kinase of the EGF receptor subfamily. *Nature* 348, 693–699.
- Ayoub, N., Goldshmidt, I., Cohen, A., 1999. Position effect variegation at the mating-type locus of fission yeast: a *cis*-acting element inhibits covariegated expression of genes in the silent and expressed domains. *Genetics* 152, 495–508.
- Ayyanathan, K., Lechner, M.S., Bell, P., Maul, G.G., Schultz, D.C., Yamada, Y., Tanaka, K., Torigoe, K., Rauscher III, F.J., 2003. Regulated recruitment of HP1 to a euchromatic gene induces mitotically heritable, epigenetic gene silencing: a mammalian cell culture model of gene variegation. *Genes Dev.* 17, 1855–1869.
- Bannister, A.J., Zegerman, P., Partridge, J.F., Miska, E.A., Thomas, J.O., Allshire, R.C., Kouzarides, T., 2001. Selective recognition of methylated lysine 9 on histone H3 by the HP1 chromo domain. *Nature* 410, 120–124.
- Beitel, G.J., Clark, S.G., Horvitz, H.R., 1990. *Caenorhabditis elegans* ras gene *let-60* acts as a switch in the pathway of vulval induction. *Nature* 348, 503–509.
- Brasher, S.V., Smith, B.O., Fogh, R.H., Nietlispach, D., Thiru, A., Nielsen, P.R., Broadhurst, R.W., Ball, L.J., Murzina, N.V., Laue, E.D., 2000. The structure of mouse HP1 suggests a unique mode of single peptide recognition by the shadow chromo domain dimer. *EMBO J.* 19, 1587–1597.
- Brenner, S., 1974. The genetics of *Caenorhabditis elegans*. *Genetics* 77, 71–94.
- Cammas, F., Herzog, M., Lerouge, T., Chambon, P., Losson, R., 2004. Association of the transcriptional corepressor TIF1beta with heterochromatin protein 1 (HP1): an essential role for progression through differentiation. *Genes Dev.* 18, 2147–2160.
- Ceol, C.J., Horvitz, R.H., 2001. *dpl-1* DP and *efl-1* E2F Act with *lin-35* Rb to antagonise Ras signaling in *C. elegans* vulval development. *Mol. Cell* 7, 461–473.
- Ceol, C.J., Horvitz, H.R., 2004. A new class of *C. elegans* synMuv genes implicates a Tip60/NuA4-like HAT complex as a negative regulator of Ras signaling. *Dev. Cell* 6, 563–576.
- Chen, N., Greenwald, I., 2004. The lateral signal for LIN-12/Notch in *C. elegans* vulval development comprises redundant secreted and transmembrane DSL proteins. *Dev. Cell* 6, 183–192.
- Chen, Z., Han, M., 2001. *C. elegans* Rb, NuRD, and Ras regulate *lin-39*-mediated cell fusion during vulval fate specification. *Curr. Biol.* 11, 1874–1879.
- Couteau, F., Guerry, F., Muller, F., Palladino, F., 2002. A heterochromatin protein 1 homologue in *Caenorhabditis elegans* acts in germline and vulval development. *EMBO Rep.* 3, 235–241.
- Cowell, I.G., Aucott, R., Mahadevaiah, S.K., Burgoyne, P.S., Huskisson, N., Bongiorno, S., Prantera, G., Fanti, L., Pimpinelli, S., Wu, R., Gilbert, D.M., Shi, W., Fundele, R., Morrison, H., Jeppesen, P., Singh, P.B., 2002. Heterochromatin, HP1 and methylation at lysine 9 of histone H3 in animals. *Chromosoma* 111, 22–36.
- Dufourcq, P., Victor, M., Gay, F., Calvo, D., Hodgkin, J., Shi, Y., 2002. Functional requirement for histone deacetylase 1 in *Caenorhabditis elegans* gonadogenesis. *Mol. Cell. Biol.* 22, 3024–3034.
- Durfee, T., Becherer, K., Chen, P.L., Yeh, S.H., Yang, Y., Kilburn, A.E., Lee, W.H., Elledge, S.J., 1993. The retinoblastoma protein associates with the protein phosphatase type 1 catalytic subunit. *Genes Dev.* 7, 555–569.
- Eissenberg, J.C., 2001. Molecular biology of the chromo domain: an ancient chromatin module comes of age. *Gene* 275, 19–29.
- Eissenberg, J.C., Elgin, S.C., 2000. The HP1 protein family: getting a grip on chromatin. *Curr. Opin. Genet. Dev.* 10, 204–210.
- Elledge, S.J., Mulligan, J.T., Ramer, S.W., Spottwood, M., Davis, R.W., 1991. Lambda YES: a multifunctional cDNA expression vector for the isolation of genes by complementation of yeast and *Escherichia coli* mutations. *Proc. Natl. Acad. Sci. U. S. A.* 88, 1731–1735.
- Ferguson, E.L., Horvitz, H.R., 1989. The multivulva phenotype of certain

- Caenorhabditis elegans* mutants results from defects in two functionally redundant pathways. *Genetics* 123, 109–121.
- Fink, C.G.G.R., 1991. Guide to yeast genetics and molecular biology. *Methods Enzymol.* 194, 3–21.
- Fire, A., Xu, S., Montgomery, M.K., Kostas, S.A., Driver, S.E., Mello, C.C., 1998. Potent and specific genetic interference by double-stranded RNA in *Caenorhabditis elegans* (see comments) *Nature* 391, 806–811.
- Fromont-Racine, M., Rain, J.C., Legrain, P., 1997. Toward a functional analysis of the yeast genome through exhaustive two-hybrid screens. *Nat. Genet.* 16, 277–282.
- Greenwald, I., Seydoux, G., 1990. Analysis of gain-of-function mutations of the *lin-12* gene of *Caenorhabditis elegans*. *Nature* 346, 197–199.
- Greenwald, I.S., Sternberg, P.W., Horvitz, H.R., 1983. The *lin-12* locus specifies cell fates in *Caenorhabditis elegans*. *Cell* 34, 435–444.
- Greil, F., van der Kraan, I., Delrow, J., Smothers, J.F., de Wit, E., Bussemaker, H.J., van Driel, R., Henikoff, S., van Steensel, B., 2003. Distinct HP1 and Su (var)3–9 complexes bind to sets of developmentally coexpressed genes depending on chromosomal location. *Genes Dev.* 17, 2825–2838.
- Henderson, S.T., Gao, D., Christensen, S., Kimble, J., 1997. Functional domains of LAG-2, a putative signaling ligand for LIN-12 and GLP-1 receptors in *Caenorhabditis elegans*. *Mol. Biol. Cell* 8, 1751–1762.
- Jacobs, S.A., Tavera, S.D., Zhang, Y., Briggs, S.D., Li, J., Eissenberg, J.C., Allis, C.D., Khorasanizadeh, S., 2001. Specificity of the HP1 chromo domain for the methylated N-terminus of histone H3. *EMBO J.* 20, 5232–5241.
- Kamath, R.S., Ahringer, J., 2003. Genome-wide RNAi screening in *Caenorhabditis elegans*. *Methods* 30, 313–321.
- Korenjak, M., Taylor-Harding, B., Binne, U.K., Satterlee, J.S., Stevaux, O., Aasland, R., White-Cooper, H., Dyson, N., Brehm, A., 2004. Native E2F/RBF complexes contain Myb-interacting proteins and repress transcription of developmentally controlled E2F target genes. *Cell* 119, 181–193.
- Lachner, M., O'Carroll, D., Rea, S., Mechler, K., Jenuwein, T., 2001. Methylation of histone H3 lysine 9 creates a binding site for HP1 proteins. *Nature* 410, 116–120.
- Lechner, M.S., Begg, G.E., Speicher, D.W., Rauscher III, F.J., 2000. Molecular determinants for targeting heterochromatin protein 1-mediated gene silencing: direct chromoshadow domain-KAP-1 corepressor interaction is essential. *Mol. Cell. Biol.* 20, 6449–6465.
- Lechner, M.S., Schultz, D.C., Negorev, D., Maul, G.G., Rauscher III, F.J., 2005. The mammalian heterochromatin protein 1 binds diverse nuclear proteins through a common motif that targets the chromoshadow domain. *Biochem. Biophys. Res. Commun.* 331, 929–937.
- Le Douarin, B., Nielsen, A.L., Garnier, J.M., Ichinose, H., Jeanmougin, F., Losson, R., Chambon, P., 1996. A possible involvement of TIF1 alpha and TIF1 beta in the epigenetic control of transcription by nuclear receptors. *EMBO J.* 15, 6701–6715.
- Lewis, P.W., Beall, E.L., Fleischer, T.C., Georlette, D., Link, A.J., Botchan, M.R., 2004. Identification of a *Drosophila* Myb-E2F2/RBF transcriptional repressor complex. *Genes Dev.* 18, 2929–2940.
- Li, Y., Kirschmann, D.A., Wallrath, L.L., 2002. Does heterochromatin protein 1 always follow code? *Proc. Natl. Acad. Sci. U. S. A.* 99 (Suppl 4), 16462–16469.
- Li, Y., Danzer, J.R., Alvarez, P., Belmont, A.S., Wallrath, L.L., 2003. Effects of tethering HP1 to euchromatic regions of the *Drosophila* genome. *Development* 130, 1817–1824.
- Linder, B., Gerlach, N., Jackle, H., 2001. The *Drosophila* homolog of the human AF10 is an HP1-interacting suppressor of position effect variegation. *EMBO Rep.* 2, 211–216.
- Lu, X., Horvitz, H.R., 1998. *lin-35* and *lin-53*, two genes that antagonize a *C. elegans* Ras pathway, encode proteins similar to Rb and its binding protein RbAp48. *Cell* 95, 981–991.
- Mains, P.E., McGhee, J.D.a.J.D., 1999. In: Hope, I.A. (Ed.), *C. elegans: a practical approach*. Oxford Univ. Pres.
- Melendez, A., Greenwald, I., 2000. *Caenorhabditis elegans lin-13*, a member of the LIN-35 Rb class of genes involved in vulval development, encodes a protein with zinc fingers and an LXCXE motif. *Genetics* 155, 1127–1137.
- Mello, C.C., Kramer, J.M., Stinchcomb, D., Ambros, V., 1991. Efficient gene transfer in *C. elegans*: extrachromosomal maintenance and integration of transforming sequences. *EMBO J.* 10, 3959–3970.
- Murzina, N., Verreault, A., Laue, E., Stillman, B., 1999. Heterochromatin dynamics in mouse cells: interaction between chromatin assembly factor 1 and HP1 proteins. *Mol. Cell* 4, 529–540.
- Myers, T.R., Greenwald, I., 2005. *lin-35* Rb acts in the major hypodermis to oppose ras-mediated vulval induction in *C. elegans*. *Dev. Cell* 8, 117–123.
- Nakayama, J., Rice, J.C., Strahl, B.D., Allis, C.D., Grewal, S.I., 2001. Role of histone H3 lysine 9 methylation in epigenetic control of heterochromatin assembly. *Science* 292, 110–113.
- Nielsen, S.J., Schneider, R., Bauer, U.M., Bannister, A.J., Morrison, A., O'Carroll, D., Firestein, R., Cleary, M., Jenuwein, T., Herrera, R.E., Kouzarides, T., 2001. Rb targets histone H3 methylation and HP1 to promoters. *Nature* 412, 561–565.
- Nielsen, P.R., Nietlispach, D., Mott, H.R., Callaghan, J., Bannister, A., Kouzarides, T., Murzin, A.G., Murzina, N.V., Laue, E.D., 2002. Structure of the HP1 chromodomain bound to histone H3 methylated at lysine 9. *Nature* 416, 103–107.
- Ogawa, H., Ishiguro, K., Gaubatz, S., Livingston, D.M., Nakatani, Y., 2002. A complex with chromatin modifiers that occupies E2F- and Myc-responsive genes in G0 cells. *Science* 296, 1132–1136.
- Peng, H., Begg, G.E., Schultz, D.C., Friedman, J.R., Jensen, D.E., Speicher, D.W., Rauscher III, F.J., 2000. Reconstitution of the KRAB-KAP-1 repressor complex: a model system for defining the molecular anatomy of RING-B box-coiled-coil domain-mediated protein–protein interactions. *J. Mol. Biol.* 295, 1139–1162.
- Poulin, G., Dong, Y., Fraser, A.G., Hopper, N.A., Ahringer, J., 2005. Chromatin regulation and sumoylation in the inhibition of Ras-induced vulval development in *Caenorhabditis elegans*. *EMBO J.* 24, 2613–2623.
- Ross, J.M., Zarkower, D., 2003. Polycomb group regulation of Hox gene expression in *C. elegans*. *Dev. Cell* 4, 891–901.
- Schultz, D.C., Ayyanathan, K., Negorev, D., Maul, G.G., Rauscher III, F.J., 2002. SETDB1: a novel KAP-1-associated histone H3, lysine 9-specific methyltransferase that contributes to HP1-mediated silencing of euchromatic genes by KRAB zinc-finger proteins. *Genes Dev.* 16, 919–932.
- Solari, F., Ahringer, J., 2000. NURD-complex genes antagonise Ras-induced vulval development in *Caenorhabditis elegans*. *Curr. Biol.* 10, 223–226.
- Spofford, J.B., 1976. Position Effect Variegation in *Drosophila*. Academic Press, New York.
- Sternberg, P.W., 1988. Lateral inhibition during vulval induction in *Caenorhabditis elegans*. *Nature* 335, 551–554.
- Sulston, J.E., Horvitz, H.R., 1977. Post-embryonic cell lineages of the nematode, *Caenorhabditis elegans*. *Dev. Biol.* 56, 110–156.
- Thiru, A., Nietlispach, D., Mott, H.R., Okuwaki, M., Lyon, D., Nielsen, P.R., Hirshberg, M., Verreault, A., Murzina, N.V., Laue, E.D., 2004. Structural basis of HP1/PXVXL motif peptide interactions and HP1 localisation to heterochromatin. *EMBO J.* 23, 489–499.
- Thomas, J.H., Ceol, C.J., Schwartz, H.T., Horvitz, H.R., 2003. New genes that interact with *lin-35* Rb to negatively regulate the *let-60* ras pathway in *Caenorhabditis elegans*. *Genetics* 164, 135–151.
- Vassallo, M.F., Tanese, N., 2002. Isoform-specific interaction of HP1 with human TAFII130. *Proc. Natl. Acad. Sci. U. S. A.* 99, 5919–5924.
- von Zellewsky, T., Palladino, F., Brunschwig, K., Tobler, H., Hajnal, A., Muller, F., 2000. The *C. elegans* Mi-2 chromatin-remodelling proteins function in vulval cell fate determination (In Process Citation) *Development* 127, 5277–5284.
- Wang, D., Kennedy, S., Conte Jr., D., Kim, J.K., Gabel, H.W., Kamath, R.S., Mello, C.C., Ruvkun, G., 2005. Somatic misexpression of germline P granules and enhanced RNA interference in retinoblastoma pathway mutants. *Nature* 436, 593–597.